

# Sensitized signalling between L-type $\text{Ca}^{2+}$ channels and ryanodine receptors in the absence or inhibition of FKBP12.6 in cardiomyocytes

Yan-Ting Zhao<sup>1†</sup>, Yun-Bo Guo<sup>1†</sup>, Lei Gu<sup>2</sup>, Xue-Xin Fan<sup>1</sup>, Hua-Qian Yang<sup>1</sup>, Zheng Chen<sup>2</sup>, Peng Zhou<sup>1</sup>, Qi Yuan<sup>2</sup>, Guang-Ju Ji<sup>2\*</sup>, and Shi-Qiang Wang<sup>1\*</sup>

<sup>1</sup>State Key Laboratory of Membrane Biology, College of Life Sciences, Peking University, 5 Yiheyuan Road, Beijing 100871, China; and <sup>2</sup>National Laboratory of Biomacromolecules, Institute of Biophysics, Chinese Academy of Sciences, 15 Datun Road, Beijing 100101, China

Received 17 September 2016; editorial decision 8 November 2016; accepted 3 December 2016; online publish-ahead-of-print 10 January 2017

Time for primary review: 49 days

## Aims

The heart contraction is controlled by the  $\text{Ca}^{2+}$ -induced  $\text{Ca}^{2+}$  release (CICR) between L-type  $\text{Ca}^{2+}$  channels and ryanodine receptors (RyRs). The FK506-binding protein FKBP12.6 binds to RyR subunits, but its role in stabilizing RyR function has been debated for long. Recent reports of high-resolution RyR structure show that the HD2 domain that binds to the SPRY2 domain of neighbouring subunit in FKBP-bound RyR1 is detached and invisible in FKBP-null RyR2. The present study was to test the consequence of FKBP12.6 absence on the *in situ* activation of RyR2.

## Methods and results

Using whole-cell patch-clamp combined with confocal imaging, we applied a near threshold depolarization to activate a very small fraction of LCCs, which in turn activated RyR  $\text{Ca}^{2+}$  sparks stochastically. FKBP12.6-knockout and FK506/rapamycin treatments increased spark frequency and LCC-RyR coupling fidelity without altering LCC open probability. Neither FK506 nor rapamycin further altered LCC-RyR coupling fidelity in FKBP12.6-knockout cells. In loose-seal patch-clamp experiments, the LCC-RyR signalling kinetics, indexed by the delay for a LCC sparklet to trigger a RyR spark, was accelerated after FKBP12.6 knockout and FK506/rapamycin treatments. These results demonstrated that RyRs became more sensitive to  $\text{Ca}^{2+}$  triggers without FKBP12.6. Isoproterenol (1  $\mu\text{M}$ ) further accelerated the LCC-RyR signalling in FKBP12.6-knockout cells. The synergistic sensitization of RyRs by catecholaminergic signalling and FKBP12.6 dysfunction destabilized the CICR system, leading to chaotic  $\text{Ca}^{2+}$  waves and ventricular arrhythmias.

## Conclusion:

FKBP12.6 keeps the RyRs from over-sensitization, stabilizes the potentially regenerative CICR system, and thus may suppress the life-threatening arrhythmogenesis.

## Keywords

Excitation-contraction coupling • FK506-binding protein • Ryanodine receptor • Calcium signalling

## 1. Introduction

$\text{Ca}^{2+}$ -induced  $\text{Ca}^{2+}$  release (CICR) is a fundamental cellular mechanism to generate and amplify intracellular  $\text{Ca}^{2+}$  signals.<sup>1,2</sup> In healthy heart cells, CICR is operated between L-type  $\text{Ca}^{2+}$  channels (LCCs) in the cell membrane/T-tubules and ryanodine receptor (RyR)  $\text{Ca}^{2+}$  release channels in the sarcoplasmic reticulum (SR).<sup>3,4</sup> The RyR-mediated SR  $\text{Ca}^{2+}$  release determines the pace and strength of myocardial contraction. Intuitively, CICR is by nature a positive feedback, and would be

expected to operate in an explosive all-or-none manner. However, the existence of solitary RyR  $\text{Ca}^{2+}$  release events,  $\text{Ca}^{2+}$  sparks,<sup>5</sup> suggests that global positive feedback among RyRs is effectively avoided such that the CICR is actually modulated precisely in a graded manner.<sup>6</sup> This paradox has been explained by the local control model, in which RyRs are under nanoscopic 'private' control by adjacent LCCs within their native  $\text{Ca}^{2+}$  release unit (CRU). Although regenerative CICR may still exist within a CRU,<sup>7,8</sup> a CRU does not respond to  $\text{Ca}^{2+}$  signals propagating from neighbouring CRUs.<sup>9–11</sup> This scenario is supported by

\* Corresponding authors. Tel: +86 10 62755002; fax: +1 501 634 3556, E-mail: wsq@pku.edu.cn; Tel: +86 10 64846720; fax: +86 10 64871293, E-mail: gj28@ibp.ac.cn

† The first two authors contributed equally.

ultrastructural studies, which show that the RyR-residing junctional SRs meet with cell membrane/T-tubules at a distance ( $\sim 15$  nm) much shorter than the inter-CRU distance.<sup>12</sup> To avoid inter-CRU crosstalk, the RyR sensitivity to  $\text{Ca}^{2+}$  triggers must be limited within a certain range.

The 12.6-kd FK506-binding protein (FKBP12.6, also known as calstabin-2) is a cardiac RyR accessory protein<sup>13,14</sup> proposed to stabilize RyR  $\text{Ca}^{2+}$  release.<sup>15,16</sup> However, the role of FKBP12.6 in RyR function has been highly controversial.<sup>17</sup> In lipid bilayer experiments, single RyRs from FKBP12.6-knockout mice or treated with rapamycin/FK506 to dissociate FKBP12.6 are found to have increased open probability and partial opening/sub-conductance.<sup>18–20</sup> However, single-channel experiments from other labs have shown that the removal of FKBP12.6 from RyRs neither alters channel activity nor prompts sub-conductance.<sup>13,21,22</sup> While it has been demonstrated that FKBP12.6 dissociation synergistically enhances the RyR response to protein kinase A (PKA)-mediated phosphorylation,<sup>15,23,24</sup> contrary evidence has shown that the PKA-induced RyR regulation does not depend on FKBP12.6.<sup>25–27</sup> In intact cardiomyocytes, some reports have shown that FK506 treatment or FKBP12.6 dissociation increases the spontaneous  $\text{Ca}^{2+}$  spark frequency and  $\text{Ca}^{2+}$  transient amplitude.<sup>20,28,29</sup> FKBP12.6 knockout mice develop severe arrhythmia that leads to sudden cardiac death during exercise.<sup>24</sup> By contrast, a later report has shown that FKBP12.6 knockout neither promotes spontaneous RyR activity nor causes ventricular arrhythmias under stress conditions.<sup>22</sup>

Recently, the high-resolution structure of mammalian RyRs has been independently reported by several research groups.<sup>30–34</sup> The structure of RyR1-FKBP12 complex shows that the BSol (HD2) domain binds to the SPRY2 domain of its neighbouring subunit, suggesting that the HD2 domain may play a role in coordinating the allosteric activity among RyR subunits. However, in FKBP-null RyR2, a large portion of HD2 is invisible, indicating that HD2 becomes flexible without FKBP. Also, FKBP12.6-knockout mice chronically develop cardiac dysfunction due to the activation of a set of signalling cascades.<sup>35</sup> These new progresses re-arouse our interest on the role of FKBP12.6 in regulating RyR  $\text{Ca}^{2+}$  release in cardiomyocytes. In the present study, we investigated the *in situ* role of FKBP12.6 in RyR function with a more rigorous experimental design. We compared the *in situ* behaviour of RyRs in wild-type and FKBP12.6 knockout cardiomyocytes, and provided direct evidence that FKBP12.6 does stabilize the *in situ* operation of RyRs in intact cardiomyocytes. FKBP12.6 loss-of-function and catecholamine stimulation synergistically over-sensitize the CICR, leading to arrhythmogenic intracellular  $\text{Ca}^{2+}$  dynamics and ventricular arrhythmias.

## 2. Methods

### 2.1 Preparation of ventricular cardiomyocytes

The investigation conforms with the Guide for Care and Use of Laboratory animals published by the US National Institutes of Health (NIH Publication No.85-23, revised 2011). Animal experiments were approved by the Institutional Animal Care and Use Committee of Peking University. Single ventricular cardiomyocytes were isolated from 3-month-old wild-type and FKBP12.6-knockout male mice,<sup>20</sup> as previously described.<sup>36</sup> Mice were anesthetized by intraperitoneally injecting with 1g/kg ethyl carbamate. The heart was immediately cut and rinsed in Tyrode solution containing (in mmol/L): 137 NaCl, 5.4 KCl, 1.2  $\text{MgCl}_2$ , 20 Hepes, 1.2  $\text{NaH}_2\text{PO}_4 \cdot 2\text{H}_2\text{O}$ , 10 glucos, 10 taurine, pH adjusted to 7.4 with NaOH. Then the aorta was cannulated to the Langendorff

apparatus and the heart was perfused through the coronary artery retrogradely with Tyrode solution at 37°C to clean the blood in vessels for 5 min. Perfusion flow rate was constant at 3mL/min for mouse hearts. With type II collagenase (200U/ml) and protease type XIV (0.35U/ml) in Tyrode's solution, the heart was perfused to be digested. When turning soft, the heart was cut into small chunks, which were then dispersed into single cells by shaking at 37°C for 3–5min, 50rpm for 3 times. Single cells were then collected by centrifuging at low speed for 1 min, and resuspended with Tyrode's solution containing 4mg/mL bovine serum albumin.  $\text{Ca}^{2+}$  concentration was restored step by step from 0.05 to 1mmol/L. Finally, cells were resuspended in extracellular solution containing (in mmol/L): 135 NaCl, 4 KCl, 1  $\text{CaCl}_2$ , 1  $\text{MgCl}_2$ , 10 Hepes, 1.2  $\text{NaH}_2\text{PO}_4 \cdot 2\text{H}_2\text{O}$ , 10 glucose, pH adjusted to 7.4 with NaOH.

### 2.2 Patch clamp

The patch clamp was made at room temperature ( $\sim 25^\circ\text{C}$ ) using an EPC7 amplifier. Cells were bathed in extracellular solution containing (in mmol/L) 135 NaCl, 4 KCl, 1  $\text{CaCl}_2$ , 1  $\text{MgCl}_2$ , 10 Hepes, 1.2  $\text{NaH}_2\text{PO}_4 \cdot 2\text{H}_2\text{O}$ , 10 glucose, pH adjusted to 7.4 with NaOH. For whole-cell patch clamp of  $I_{\text{Ca,L}}$  recording, 15  $\mu\text{M}$  tetrodotoxin and 4 mM 4-aminopyridine were added in the extracellular solution. A glass pipette with a resistance ( $R_p$ ) of 2–3 M $\Omega$  was filled with (in mmol/L) 110 CsCl, 6  $\text{MgCl}_2$ , 5  $\text{Na}_2\text{ATP}$ , 10 Hepes, 15 TEA-Cl, 0.2 Fluo-4 pentapotassium, pH adjusted to 7.2 with CsOH. In loose-seal experiments, cells were loaded with fluo-4-AM and the pipette electrode with  $R_p$  of 4–6 M $\Omega$  was filled with (in mmol/L) 120 TEA-Cl, 10 Hepes, 0.01 TTX, 20  $\text{CaCl}_2$  and 0.01 FPL64176, pH adjusted to 7.4 with TEA-OH, and was gently pressed onto the cell surface to form a low-resistance seal ( $R_s = 20\text{--}30$  M $\Omega$ ). The patch membrane voltage ( $V_p$ ) was determined based on the resting potential (RP) and command voltage ( $V_{\text{com}}$ ) by  $V_p = \text{RP} - V_{\text{com}}(R_s - R_p)/R_s$ .

### 2.3 Confocal $\text{Ca}^{2+}$ imaging

$\text{Ca}^{2+}$  imaging was recorded as previously described.<sup>37</sup> In whole-cell patch clamp experiments, the  $\text{Ca}^{2+}$  indicator Fluo-4 pentapotassium salt (200 $\mu\text{mol/L}$ ) was already included in the pipette solution. In loose-patch and  $\text{Ca}^{2+}$  wave experiments, cells were loaded with 10 $\mu\text{mol/L}$  fluo-4-AM (Invitrogen) in 37°C for 5 min in extracellular solution. After the incubation, cells were washed with extracellular solution.  $\text{Ca}^{2+}$  imaging was recorded with a Zeiss LSM-510 inverted confocal microscope (Carl Zeiss) with 488 nm laser excitation and a 40X 1.3 N.A. oil-immersion objective. All images were acquired along the long axis of cells in line-scan mode at a sampling rate of 0.768 ms/line for sparklet-spark experiments and 15.36 ms/line for other experiments. Local  $[\text{Ca}^{2+}]$  was determined by the formula  $[\text{Ca}^{2+}] = k_d \cdot R / (k_d / C_0 + 1 - R)$ , where R is the relative fluo-4 fluorescence normalized by the resting level,  $k_d = 1.1$   $\mu\text{M}$  is the apparent dissociation constant of fluo-4, and  $C_0 = 100\text{nM}$  is the resting  $\text{Ca}^{2+}$  concentration.

We measured the sparklet-spark latency only for the first spark triggered during a depolarization. The latency was determined by tracing back from the upstroke of a spark to the first datum point that fell below the SD of baseline. Given that the LCC-RyR coupling is a stochastic process, a significant portion of the latency data, represented by the first bar of the latency histogram, were too short for a sparklet to be visually identified (for example, see the right panel of Figure 3A). However, this does not influence the reliability of the latency histogram, which follows an exponential distribution. The apparent rate constant ( $k$ ) for RyRs to respond to LCC  $\text{Ca}^{2+}$  sparklets was determined by fitting the

distribution with the formula  $N = N_0 e^{-kt}$ , where  $N$  is the number of observations and  $N_0$  is the  $N$  when  $t = 0$ .

## 2.4. Electrocardiography

Mice were lightly anesthetized with isoflurane (1%) and placed supine on a heated pad of 37°C. Needle ECG electrodes were placed under the skin to record from a Lead I configuration. After a 20-min baseline period, epinephrine (2 mg/kg) was injected intraperitoneally. Arrhythmias were defined as either non-sustained ventricular tachycardia (VT) (e.g. a series of 4–10 consecutive repetitive ventricular ectopic beats) or sustained VT (e.g. a run of 11 or more consecutive repetitive ventricular ectopic beats).

## 2.5 Data analysis and statistics

All data are expressed as mean  $\pm$  SE unless otherwise indicated. The linear mixed effects model (by R program and *lme4*) or  $\chi^2$  test, where appropriate, were applied for unpaired samples to determine statistical differences. Bonferroni correction was applied when more than two groups were compared to the same control. Curve fitting was performed using Sigmaplot software (Systat Software, Inc). Fitted data were compared using the  $u$  test.  $P < 0.05$  was considered statistically significant.

## 3. Results

### 3.1 FKBP12.6-knockout increases LCC-RyR coupling fidelity

In order to test the effect of FKBP12.6 on the *in situ* RyR response to LCC  $\text{Ca}^{2+}$  influx, we sought to trigger discrete  $\text{Ca}^{2+}$  sparks by minimal LCC activation in ventricular cardiomyocytes from wild-type (WT) and FKBP12.6 knockout (FKO) mice. In cardiomyocytes loaded with the  $\text{Ca}^{2+}$  indicator fluo-4, we recorded LCC  $\text{Ca}^{2+}$  current ( $I_{\text{LCC}}$ ) using the whole-cell patch clamp technique (Figure 1A). Neither the  $I_{\text{LCC}}$  density (Figure 1B) nor its voltage dependence (Figure 1C) differed between WT and FKO. By Boltzmann fitting of the activation curves, we determined that the probability of LCC activation at -40 mV in both FKO and WT groups was only around 0.003 (Figure 1C). The low probability of LCC openings at the near-threshold depolarization allowed us to compare the frequency of solitary RyR  $\text{Ca}^{2+}$  sparks triggered probabilistically by LCCs (Figure 1D). We found that the frequency of  $\text{Ca}^{2+}$  sparks triggered by the depolarization from -50 to -40 mV was significantly higher in FKO than in WT (Figure 1E). Due to the low probability of LCC openings, the majority of  $\text{Ca}^{2+}$  spark should be activated by a single LCC, confirming that the  $\text{Ca}^{2+}$  influx through a single LCC is capable of triggering a  $\text{Ca}^{2+}$  spark.<sup>38</sup> Because the  $I_{\text{LCC}}$  at -40 mV ( $I_{-40}$ ), calculated based on Boltzmann fitting, was comparable between FKO and WT groups (Figure 1F), the higher frequency of  $\text{Ca}^{2+}$  sparks in FKO reflected increased RyR response to LCCs. We therefore derived the LCC-RyR coupling fidelity by calculating the  $F_{\text{spark}}$  per unit  $I_{-40}$  ( $F_{\text{spark}}/I_{-40}$ , Figure 1G), and found that the coupling fidelity was significantly higher in FKO than in WT.

To exclude any possible influence of SR  $\text{Ca}^{2+}$  load on the above results, we measured the  $\text{Ca}^{2+}$  transient induced by rapidly applying 20 mM caffeine, which opens RyRs simultaneously and allows stored  $\text{Ca}^{2+}$  in the SR to diffuse into the cytosol. The caffeine-induced  $\text{Ca}^{2+}$  transient amplitude was the same in WT and FKO cells (Figure 1H), indicating that the SR load was not altered in FKO cells. It has been reported that the gain of excitation–contraction coupling is increased by

early reverse  $\text{Na}^+/\text{Ca}^{2+}$  exchange (NCX) activated during depolarization.<sup>39</sup> To avoid possible involvement of NCX, we applied minimal depolarization (from -50 to -40 mV) when the  $\text{Na}^+$  channels were blocked by tetrodotoxin. Therefore, under our experimental conditions, the increased coupling fidelity in the FKO group was attributable to increased responsiveness of RyRs to  $I_{\text{LCC}}$ .

### 3.2 FK506 and rapamycin increases LCC-RyR coupling fidelity in WT but not FKO cells

In heart cells, both FKBP12 and FKBP12.6 bind to RyRs but their binding affinity differs.<sup>13,40,41</sup> In order to check whether FKBP12 has a compensatory effect to FKBP12.6 knockout, we performed pharmacological experiments with 30  $\mu\text{mol/L}$  FK506 and 10  $\mu\text{mol/L}$  rapamycin, both are known to dissociate FKBP from RyRs.<sup>18,19</sup> Agreeing with previous reports,<sup>19,28,42</sup> neither FK506 nor rapamycin changed the  $I_{\text{LCC}}$  (see Supplementary material online, Figure S1). We found that both FK506- and rapamycin-treatments increased the LCC-RyR coupling fidelity ( $F_{\text{spark}}/I_{\text{LCC}}$ ) of WT cardiomyocytes to the same extent as that caused by FKO (comparing Figure 2A with Figure 1G). In contrast, neither treatment could further change the  $F_{\text{spark}}/I_{\text{LCC}}$  in FKO cells (Figure 2B), suggesting that FKBP12 did not exert a compensatory effect. The fact that FKBP12.6 knockout and FK506-/rapamycin-treatment have the same effect on  $F_{\text{spark}}/I_{\text{LCC}}$  indicated that the knockout-/treatment-induced increase in RyR responsiveness was fully attributable to FKBP12.6 dissociation.

### 3.3 FKBP12.6 absence accelerates RyR response to a single LCC

The whole-cell detection of  $\text{Ca}^{2+}$  sparks usually involves out-of-focus events, and may also induce global feedback of CICR, particularly when the RyRs are sensitized. In order to further quantify the role of FKBP12.6 on LCC-RyR signalling, we visualized  $\text{Ca}^{2+}$  sparklets from LCCs and triggered  $\text{Ca}^{2+}$  sparks from RyRs by confocal imaging by loose-seal patch clamp.<sup>37,38</sup> When the patched membrane was depolarized from resting potential (RP) to -10 mV, line-scan imaging focused at the pipette tip detected that  $\text{Ca}^{2+}$  sparklets from LCCs (blue arrows in Figure 3A) activated  $\text{Ca}^{2+}$  sparks from RyRs (red arrows in Figure 3A) in a stochastic manner. For those  $\text{Ca}^{2+}$  sparklets that successfully triggered  $\text{Ca}^{2+}$  sparks, the latency from the onset of an LCC sparklet to the takeoff of a triggered RyR spark varied, exhibiting exponential distributions in both WT and FKO groups (Figure 3B). The apparent rate constant ( $k$ ) for RyRs to respond to LCC sparklets was then determined by fitting the distributions with the formula

$$N = N_0 e^{-kt},$$

where  $N$  is the number of observations and  $N_0$  is the  $N$  when  $t = 0$ . The fitting showed that the  $k$  was 29% higher in FKO cells than in WT cells (Figure 3C), indicating that the LCC-RyR signalling was accelerated after FKBP12.6 knockout.

In order to exclude any chronic compensatory effect of FKBP12.6 knockout, we further measured the LCC-RyR coupling latency with FK506 or rapamycin treatment in WT cardiomyocytes to acutely dissociate FKBP12.6 from RyR. Similarly with FKO cells, both FK506 and rapamycin accelerated LCC-RyR coupling rate (Figure 3D–F).

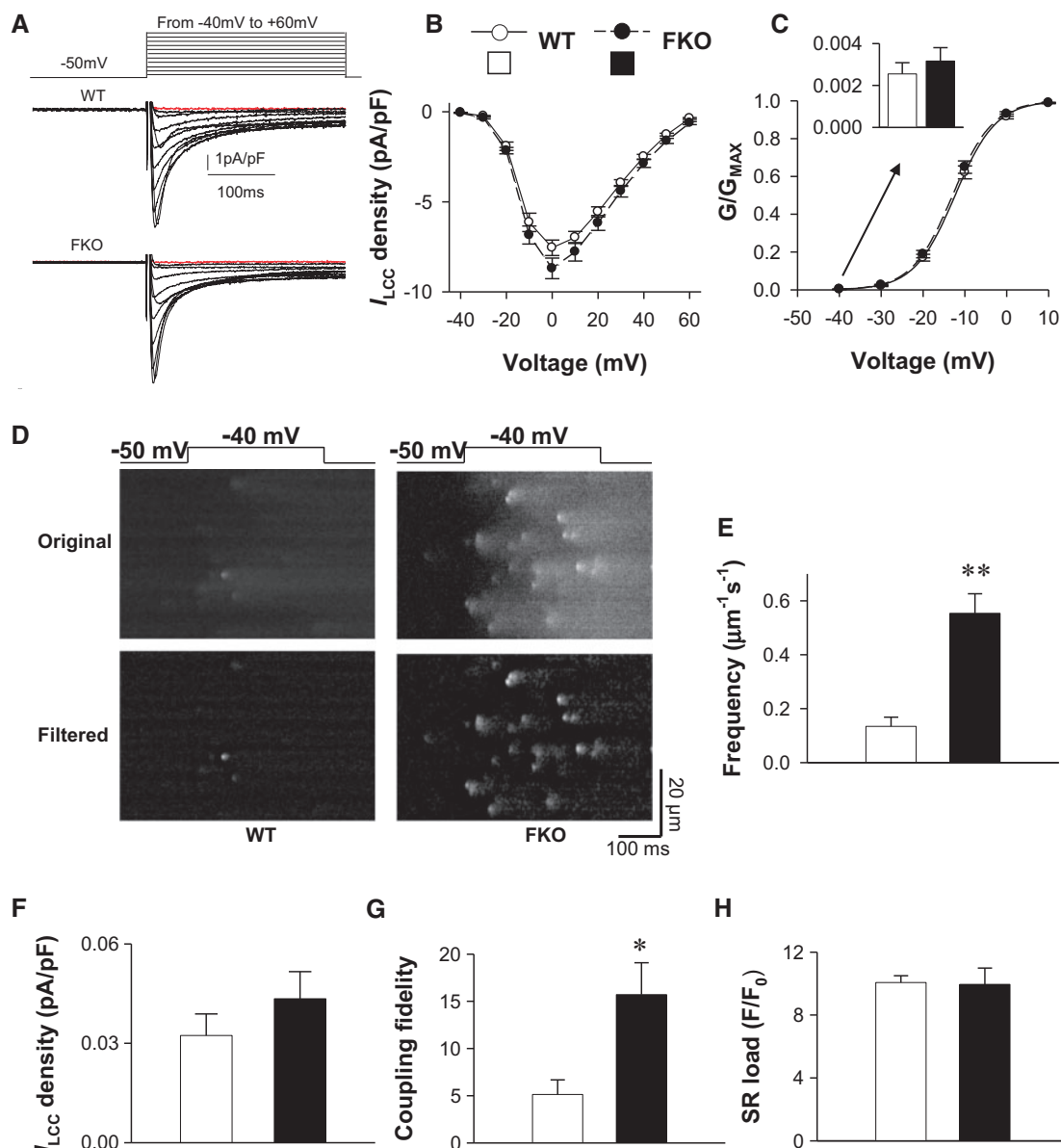


**Figure 1** FKBP12.6 knockout increases LCC-RyR coupling probability by near-threshold depolarization. (A) Currents were triggered from -50 mV to different depolarizations (-40 mV to +60 mV) in WT and FKO cardiomyocytes. Red curves were currents triggered at to -40 mV. (B) Whole cell  $I_{LCC}$  density in WT and FKO cardiomyocytes. (C) The activation curves derived from the  $I_{LCC}$ -V curves in (B). The  $G/G_{MAX}$  at -40 mV (insert) was determined by fitting the data with Boltzmann equation  $G/G_{MAX} + 1/[1 + \exp(a-bV)]$ , where  $a$  and  $b$  are fitting constants. (D) Representative recordings showing that a 300 ms depolarization from -50 to -40 mV (upper panels) under the whole-cell patch clamp condition activates  $Ca^{2+}$  sparks in a probabilistic manner (middle panels). In order to identify individual sparks clearly, the original images were high-pass filtered by subtracting a smoothed image (kernel size  $10 \mu\text{m} \times 50 \text{ms}$ ) (lower panels). (E) The frequency of  $Ca^{2+}$  sparks at -40 mV in WT and FKO cardiomyocytes. Data from  $\geq 23$  cells from  $\geq 6$  mice in each group. (F) The  $I_{LCC}$  density at -40 mV was determined by  $I_{LCC} = G(V - V_R)$ , where  $G$  is the LCC conductance,  $V$  is the membrane potential and  $V_R$  is the reverse potential. (G) The frequency of  $Ca^{2+}$  sparks per unit  $I_{LCC}$  (coupling fidelity =  $F_{spark}/I_{LCC}$ ). The unit for  $F_{spark}/I_{LCC}$  is  $\mu\text{m}^{-1} \cdot \text{s}^{-1} \cdot \text{pA}^{-1} \cdot \text{pF}$ . (H) SR  $Ca^{2+}$  load measured as the amplitude of  $Ca^{2+}$  transients evoked by 20 mM caffeine under the whole-cell patch clamp. Data were from  $\geq 7$  cells from 3 mice in each group. \* $P < 0.05$  and \*\* $P < 0.01$  vs. WT.

### 3.4 $\beta$ -adrenergic stimulation further accelerates RyR response to a single LCC in FKO cells

Next, we sought to probe whether the absence of FKBP12.6 influences the *in situ* RyR response to the stimulation of  $\beta$ -adrenergic receptors ( $\beta$ ARs). In the whole-cell experiment,  $\beta$ AR stimulation will increase the

LCC open probability, making it unreliable to quantify RyR response by near-threshold coupling fidelity ( $F_{spark}/I_{LCC}$ ). By the loose-patch activation of  $Ca^{2+}$  sparks, we measured the coupling latency from LCC sparklets to RyR sparks when  $\beta$ ARs was activated by  $1 \mu\text{mol/L}$  isoproterenol (ISO, Figure 4A). Normalized exponential fitting of the LCC-RyR latency distribution (Figure 4B) showed that the LCC-RyR coupling latency was



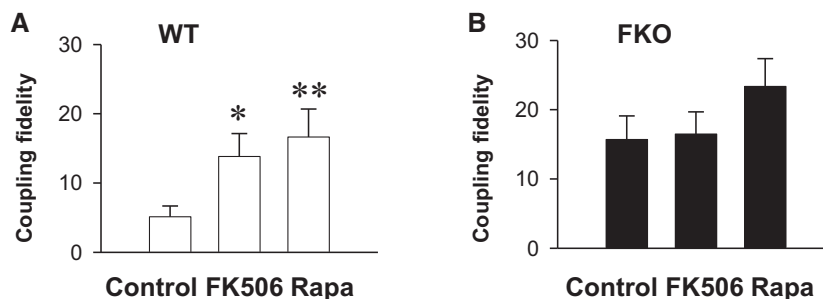


**Figure 2** FK506 and rapamycin increases LCC-RyR coupling probability in WT but not FKBP12.6 knockout cells. (A) The effect of FK506 and rapamycin treatment on coupling fidelity in WT. (B) The effect of FK506 and rapamycin treatment on coupling fidelity in FKO. Data from  $\geq 23$  cells from  $\geq 6$  mice in each group. \* $P < 0.05$  and \*\* $P < 0.01$  vs. Control.

shortened after ISO treatment and further shortened in the ISO-treated FKO group. Compared with the WT group, the  $k$  of RyR response was accelerated by 78% in the ISO-treated FKO group (Figure 4C). Because ISO and FKO alone increased the  $k$  by 33 and 29%, respectively, the 78% increase of  $k$  indicated that FKBP12.6 knockout and  $\beta$ AR stimulation additively sensitize the RyR response to  $\text{Ca}^{2+}$  triggers.

### 3.5 Destabilization of CICR due to the absence of FKBP12.6

We then tested the stability of the CICR system at the whole-cell level by analysing intracellular  $\text{Ca}^{2+}$  activity after 30 pulses of field stimulation at 2 Hz in mouse cells. To avoid the possible toxic effects of laser scanning, we only imaged the cells during and after the last three beats. WT cells without ISO treatment usually displayed synchronized  $\text{Ca}^{2+}$  transients with clean diastolic background between successive stimulations and thereafter (Figure 5A, upper). The treatment with 1  $\mu\text{M}$  ISO moderately increased the chance for WT cells to develop  $\text{Ca}^{2+}$  waves after field stimulation (Figure 5B white and striped white bars). Although FKO cells without ISO treatment also tended to keep regular  $\text{Ca}^{2+}$  transients, most FKO cells treated with ISO fell into chaotic  $\text{Ca}^{2+}$  waves (Figure 5A, lower and Figure 5B grey and striped grey bars). This result suggested that the CICR system loses stability under  $\beta$ -adrenergic stimulation in the absence of FKBP12.6.

To further test whether the cellular alterations described above predispose FKBP12.6 knockout mice to cardiac arrhythmias, we performed electrocardiography (ECG) in WT and FKO mice before and after catecholaminergic challenge by intraperitoneal administration of epinephrine (Epi) (Figure 5C). At basal condition, neither WT nor FKO displayed ventricular arrhythmias. Catecholaminergic challenge elicited few arrhythmic events in WT mice, but led to more frequent ventricular arrhythmias in FKO mice (Figure 5D).

## 4. Discussion

FK506-binding proteins, including FKBP12 and FKBP12.6, are important modulators of RyRs.<sup>13,43,44</sup> In heart cells, FKBP12.6 binds RyRs with a much higher affinity than FKBP12.<sup>13,40,41,45</sup> In the present study, we investigated the role of FKBP12.6 in modulating RyR  $\text{Ca}^{2+}$  release using FKBP12.6-knockout mice and FK506/rapamycin pharmacology. Either of these two experimental systems may have limitations: the acute

treatment with FK506/rapamycin may contaminate with FKBP12 effect, while FKBP12.6-knockout strategy may involve chronic compensation. Therefore, we have exerted both experimental systems for complementary. The acute treatment with FK506/rapamycin excluded the chronic compensation and adaptation possibly associated with gene manipulation, but might involve an effect of FKBP12 dissociation. This latter concern was eliminated by the FKBP12.6 knockout results, which were fully attributable to the absence of FKBP12.6. Both lines of evidence demonstrated that FKBP12.6 dissociation (i) increased the CICR sensitivity and activation probability of RyRs, (ii) further sensitized RyRs under  $\beta$ -adrenergic stimulation, and (iii) elevated the risk for heart cells to develop arrhythmogenic  $\text{Ca}^{2+}$  activity. Therefore, the presence of FKBP12.6 should play an important role in stabilizing the CICR system in intact heart cells.

In previous studies, one of the problems keeping the role of FKBP12.6 from clarification is that RyRs are intracellular channels inaccessible to direct electrophysiological measurements. Although lipid bilayers have been widely used to study the interaction between FKBP12.6 and RyRs, the experimental settings vary greatly from lab to lab. For example, an experiment supporting FKBP12.6-modulation of RyR was done in the presence of  $\text{Mg}^{2+}$  and 50 mmol/L *trans*(luminal)-side  $\text{Ca}^{2+}$ ,<sup>24</sup> whereas counteracting data were collected with symmetrical high concentration of  $\text{K}^+$  without  $\text{Mg}^{2+}$ .<sup>22</sup> Despite the differences in ionic composition, lipid bilayer experiments cannot reconstruct the native environment of interacting proteins, such as calsequestrin, junctin, and triadin. Therefore, the results in lipid bilayers may not necessarily represent the *in situ* effect of FKBP12.6.

In intact cardiomyocytes, early reports have shown that spontaneous  $\text{Ca}^{2+}$  spark amplitude is either decreased<sup>19</sup> or unchanged<sup>28</sup> after FK506 treatment. However, studies in FKO mice showed that  $\text{Ca}^{2+}$  spark amplitude is either increased<sup>22</sup> or unchanged<sup>31</sup> in the absence of FKBP12.6. We noticed that, in reports showing increased  $\text{Ca}^{2+}$  spark amplitude, spark duration and full-width at half-maximum (FWHM) were also increased.<sup>22</sup> Given that the  $\text{Ca}^{2+}$  spark frequency was increased by several folds, FKO cells display a lot of overlapping sparks and local wavelets,<sup>20,29</sup> which caused overestimation of  $\text{Ca}^{2+}$  spark amplitude, duration, and FWHM. In the present study, we did not measure overlapping sparks. Our measurement of spontaneous sparks showed that spark amplitude, time-to-peak, FWHM, and full-duration at half-maximum were comparable between WT and FKO cells (see Supplementary ma

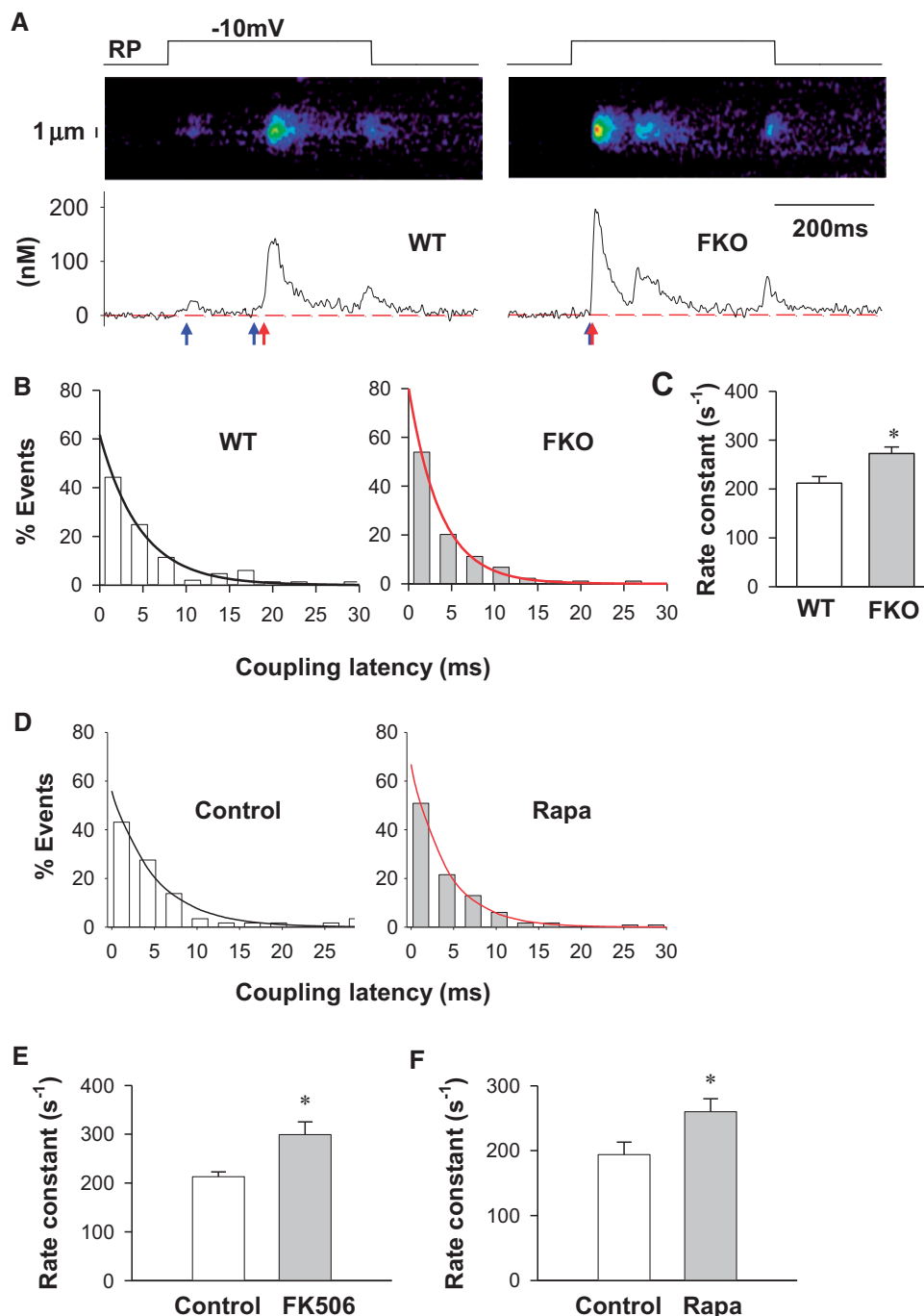


**Figure 3** FKBP12.6 dysfunction accelerates the kinetics of LCC-RyR coupling. (A) Representative recordings from WT and FKO groups showing that depolarization to  $-10\text{ mV}$  from resting potential (RP) (upper panels) triggered  $\text{Ca}^{2+}$  sparklets and  $\text{Ca}^{2+}$  sparks (middle panels for images and lower panels for time profiles) in a probabilistic manner. The blue and red arrows indicate the beginning of  $\text{Ca}^{2+}$  sparklets and  $\text{Ca}^{2+}$  sparks, respectively. (B) Distributions (bars) and exponential fittings (curves) of the coupling latency in WT and FKO groups. (C) Rate constants of LCC-RyR coupling in WT and FKO. (D) Distributions (bars) and exponential fittings (curves) of the coupling latency in WT under control and rapamycin-treated conditions. (E) Rate constants of LCC-RyR coupling in WT under control and FK506-treated conditions. (F) Rate constants of LCC-RyR coupling in WT under control and rapamycin-treated conditions. Data from  $\geq 86$  recordings in cells from  $\geq 15$  mice in each group.  $*P < 0.05$  vs. WT or control.

terial online, Figure S2). However, when the RyR  $\text{Ca}^{2+}$  release was activated by native LCC current under the loose-patch and whole-cell depolarization conditions, we did find that the rate constant and probability of spark activation were significantly increased when FKBP12.6 was

absent, presumably due to increased open probability of RyRs. These data indicated that the kinetic change of RyR activation is not reflected in spontaneous  $\text{Ca}^{2+}$  sparks. The mixture of in-focus and off-focus  $\text{Ca}^{2+}$  release events in spontaneous sparks makes it difficult to quantify

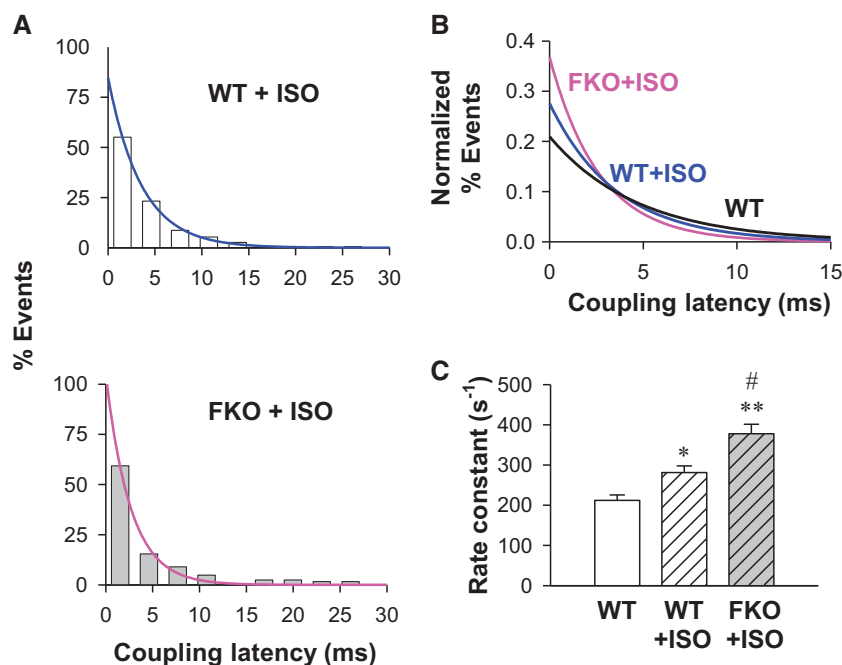


**Figure 4** FKBP12.6 knockout and  $\beta$ -adrenergic stimulation additively sensitize LCC-RyR coupling. (A) Distributions (bars) and exponential fittings (curves) of the coupling latency in WT (upper), FKO (lower) cardiomyocytes bathed in 1  $\mu$ M ISO. (B) Comparison of normalized curves fitting in WT (black), WT + ISO (blue) and FKO + ISO (purple) groups. (C) Rate constants of LCC-RyR coupling in WT, WT + ISO and FKO + ISO groups. Data from  $\geq 104$  recordings in cells from  $\geq 15$  mice. \* $P < 0.05$  and \*\* $P < 0.01$  vs. WT; # $P < 0.05$  vs. WT + ISO.

RyR properties. Therefore, the difference in experimental design at least partially explains why the role of FKBP12.6 in stabilizing RyR  $\text{Ca}^{2+}$  release is not detected in some studies.

In the present study, the triggering of RyR  $\text{Ca}^{2+}$  sparks by unitary LCC current made it more feasible than previously to investigate RyR  $\text{Ca}^{2+}$ -sensitivity in intact cells. Our LCC-RyR coupling experiments provided two lines of evidence for the enhanced  $\text{Ca}^{2+}$  sensitivity of RyRs after FKBP12.6 knockout or FK506/rapamycin treatment: (i) an increased probability for LCC openings to activate RyRs, and (ii) an accelerated response of RyRs to single LCC  $\text{Ca}^{2+}$  influx. Given that an LCC opening has limited lifetime, a quicker response implies that a RyR has a higher chance of being activated before the LCC closes. Therefore, the accelerated coupling kinetics agreed well with the increased probability of LCC-RyR coupling. Both measurements provided unequivocal evidence that RyRs are sensitized to  $\text{Ca}^{2+}$  triggers after FKBP12.6 dissociation. In other words, the sensitivity of RyR activation is under tonic suppression by FKBP12.6 under physiological conditions.

Guo et al.<sup>41</sup> reported that only  $<20\%$  FKBP12.6 binding sites on RyRs are occupied by FKBP12.6 in mouse heart cells. As each RyR has 4 FKBP12.6 binding sites on its 4 subunits,  $<41\%$  RyRs would bind with one FKBP12.6 molecule,  $<15\%$  with 2,  $<2.5\%$  with 3, and only  $<0.16\%$  RyRs would be fully occupied by FKBP12.6. The robust effect of FKBP12.6 knockout could not be explained if multiple FKBP12.6 binding was required to modify RyR behaviour. Therefore, we infer that single occupation of the FKBP12.6-binding sites should be effective in stabilizing RyR function. Based on the recent reports of RyR structure,<sup>31–34</sup> FKBP is inserted into the gap between JSol (handle) domain and SPRY triangle. Structural comparison using the data of RyR1-FKBP12 complex<sup>32</sup> and FKBP-null RyR2<sup>34</sup> suggested that the insertion of FKBP may adjust the

positioning of certain domains such that the BSol (HD2) domain can be anchored onto the SPRY2 domain of the neighbouring protomer (nSPRY2) (Figure 6A and B). The putative HD2-nSPRY2 interaction thus provides a possible mechanism for inter-subunit coordination (Figure 6C). In this scenario, a single-subunit occupation of FKBP12.6 would be expected to stabilize 2 adjacent subunits of a RyR, and a 20% occupation of FKBP12.6-binding sites would stabilize  $\sim 59\%$  ( $41 + 15 + 2.5 + 0.16$ )% RyRs. This prediction explains the robust effect of FKBP12.6 knockout on LCC-RyR signalling.

The role of FKBP12 in modulating RyRs in cardiac cells is another emerging controversy. It is shown that FKBP12 binds RyRs with very low affinity in heart cells,<sup>41</sup> and overexpression of FKBP12 reduces the sensitivity of RyRs to  $\text{Ca}^{2+}$ .<sup>46</sup> However, it has been reported that FKBP12 is a high affinity activator of RyR2, sensitizing RyRs to cytosolic  $\text{Ca}^{2+}$ .<sup>47</sup> In the present study, we showed that FK506 did not further influence coupling fidelity in FKBP12.6-null cardiomyocytes, suggesting that FK506-induced FKBP12 dissociation had little effects on RyR sensitivity in intact ventricular cardiomyocytes.

The sympathetic system regulates heart function through ARs. It has been reported that FKBP12.6 knockout mice develop severe arrhythmia that leads to sudden cardiac death during exercise, well mimicking catecholaminergic polymorphic ventricular tachycardia.<sup>24,25</sup> However, many experiments do not support the above idea.<sup>17,26,27</sup> It has been shown that FKBP12.6 knockout neither promotes RyR activity nor causes ventricular arrhythmias under stress conditions.<sup>22</sup> To determine whether and how FKBP12.6 interferes with the  $\beta$ -AR regulation of RyRs, we compared the effect of ISO, a selective  $\beta$ -AR agonist, on the LCC-RyR signalling kinetics in WT and FKO cardiomyocytes. In both groups, ISO treatment accelerated the coupling rate constant. The result that  $\beta$ -AR

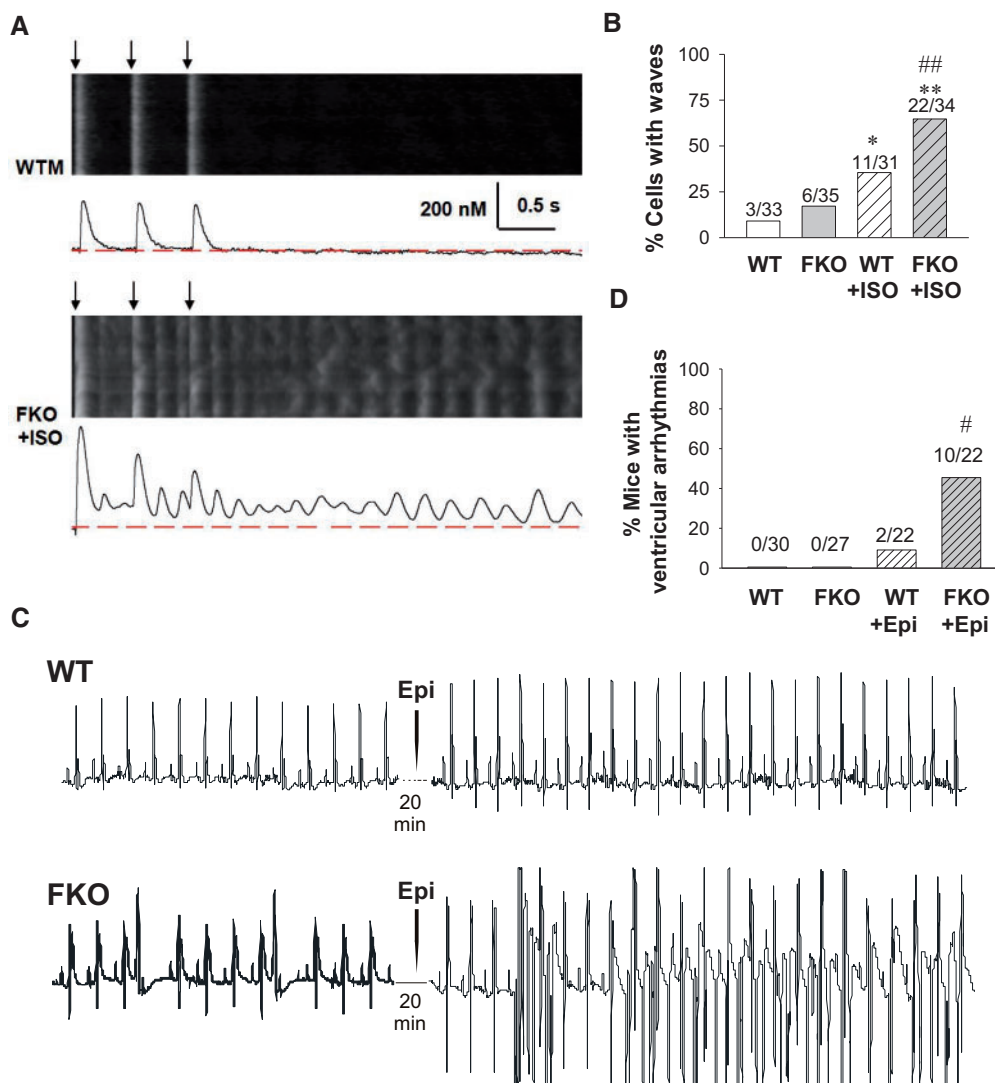


**Figure 5** FKBP12.6 knockout increases the global  $\text{Ca}^{2+}$  release after field stimulation with ISO treatment and the ventricular arrhythmias after catecholaminergic stimulation in mice. (A) Representative confocal images and their time profiles of the last 3  $\text{Ca}^{2+}$  transients of 30 pulses of 2 Hz stimulation in WT (upper) and ISO-treated FKO (lower) cardiomyocytes. Black arrows denote the timing of field stimulations. (B) Percentage of cells displaying  $\text{Ca}^{2+}$  waves in mouse cells under 2-Hz stimulation. The number of observations in each group is marked in the panels. \* $P < 0.05$  and \*\* $P < 0.01$  vs. WT; ### $P < 0.01$  vs. WT + ISO. (C) Representative echocardiographic recordings from WT (upper) and FKO (lower) mice before and after epinephrine (Epi) treatment. (D) Percentage of mice with ventricular arrhythmias. #  $P < 0.05$  vs. WT + Epi.

regulation further accelerated the LCC-RyR signalling kinetics in FKO cells provided *in situ* evidence at the molecular level that  $\beta$ -AR stimulation is able to sensitize  $\text{Ca}^{2+}$ -induced RyR activation via an FKBP12.6-independent mechanism. Because FKBP12.6 absence *per se* sensitizes RyR activation, our results indicated that FKBP12.6-dependent and  $\beta$ -AR-mediated FKBP12.6-independent sensitization mechanisms cooperate in an additive manner in ISO-treated FKO cells.

The effect of FKBP12.6 on RyR2  $\text{Ca}^{2+}$  release has also been investigated previously by overexpressing the FKBP12.6 gene in rabbit<sup>16,48</sup> or rat<sup>49</sup> cardiac myocytes, and by FKBP12.6-overexpression mouse models<sup>50-54</sup>. FKBP12.6 overexpression decreases spontaneous  $\text{Ca}^{2+}$  spark frequency<sup>48,49,51</sup> and SR  $\text{Ca}^{2+}$  leak,<sup>16</sup> which in turn increases SR  $\text{Ca}^{2+}$  load<sup>16,48,49</sup> and  $\text{Ca}^{2+}$  transient peak.<sup>48,49</sup> FKBP12.6 overexpression also increases the degree of synchronicity of SR  $\text{Ca}^{2+}$  release.<sup>48</sup> Taken

together, FKBP12.6 overexpression stabilizes RyR2 and prevents arrhythmogenic SR  $\text{Ca}^{2+}$  leak at the cellular level, which is in agreement with our findings by FKO cells. Furthermore, FKBP12.6-overexpressed mouse model shows improved cardiac function after myocardial infarction,<sup>50</sup> decreased ventricular tachycardia after catecholaminergic stimulation,<sup>51</sup> ameliorated post-thoracic aortic constriction (TAC) survival rates,<sup>52</sup> protection against maladaptive left ventricular hypertrophy and reduced ventricular arrhythmias after TAC.<sup>53</sup> The results from FKBP12.6 overexpression mouse model and our FKBP12.6 knockout model double confirmed that FKBP12.6 exerts a protective effect on heart function.

CICR is intrinsically a positive feedback loop, and would be expected to be explosive.<sup>55</sup> However, the  $\text{Ca}^{2+}$  release of RyRs in heart cells is modulated precisely in the forms of both global  $\text{Ca}^{2+}$  transients and local  $\text{Ca}^{2+}$  sparks. As the key mechanism to avoid the self-excitation of CICR



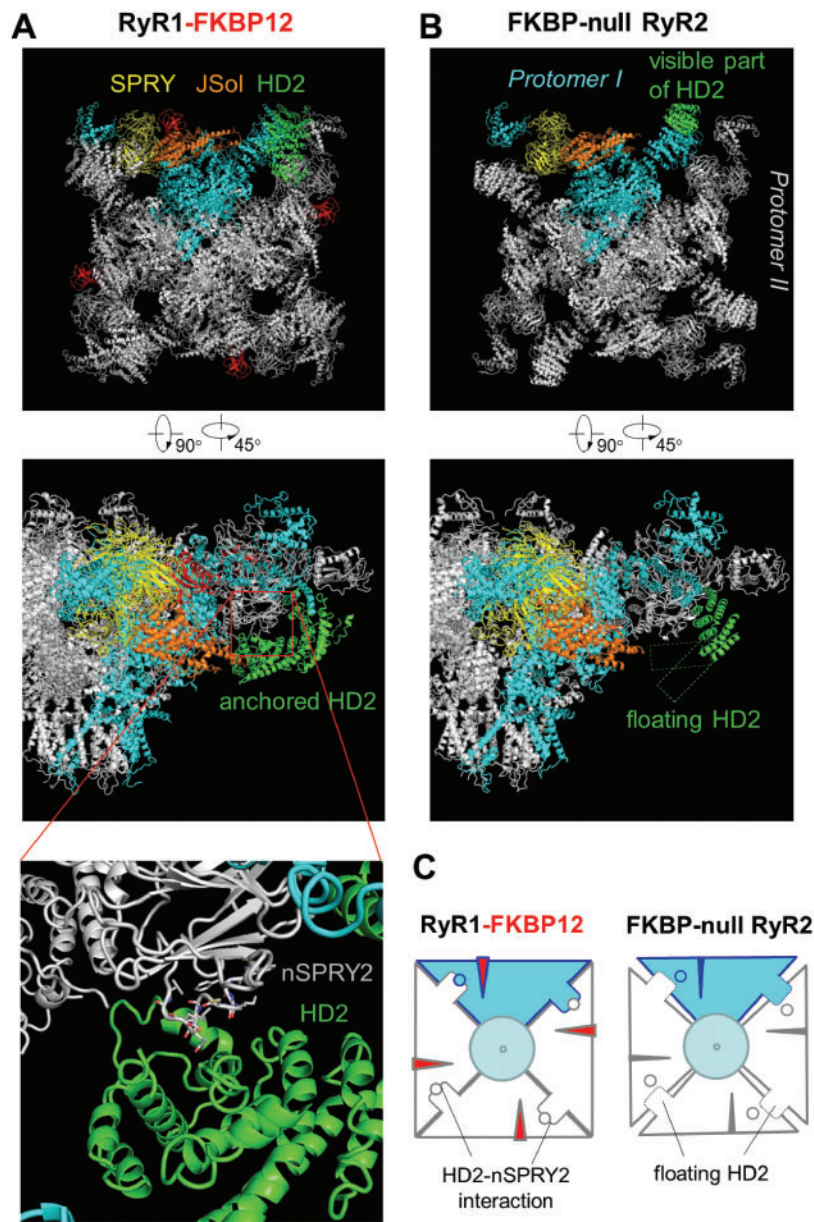


**Figure 6** Structural comparison between RyR1-FKBP12 complex and FKBP-null RyR2. The images were generated based on the original structural data from Zalk et al.<sup>32</sup> for RyR1 and from Peng et al.<sup>34</sup> for RyR2. (A) In RyR1-FKBP12 complex, the JSol (HD2) domain potentially interacts with the SPRY2 domain of the neighbouring protomer (nSPRY2). (B) In FKBP-null RyR2, the HD2 domain is largely invisible, indicating that it may be floating without HD2-nSPRY2 interaction. (C) A hypothetical scheme based on the above information illustrating that the putative HD2-nSPRY2 interaction provides a possible mechanism for FKBP12 to coordinate the allosteric activity among protomers. This HD2-nSPRY2 interaction may become destabilized without FKBP.

in heart cells, RyRs and LCCs are clustered to form discrete CRUs.<sup>12,56,57</sup> Within each CRU, the  $\text{Ca}^{2+}$  influx through LCCs travels across a  $\sim 15$  nm junctional cleft, and activates RyRs in a stochastic manner.<sup>58</sup> Between CRUs, however, the longer distance prevents crosstalk between adjacent CRUs.<sup>12</sup> In this scenario, the RyR sensitivity must be limited within a certain dynamic range, or stability margin, such that the RyRs respond promptly to  $\text{Ca}^{2+}$  signals from LCCs but not to those from adjacent CRUs. Based on our findings,  $\beta$ -AR stimulation and FKBP12.6 dissociation both sensitized RyRs. When either of these

factors act solo, the chance of generating regenerative  $\text{Ca}^{2+}$  activity is kept at a low level comparable with that in wild-type/control conditions, suggesting that moderate sensitization by FKBP12.6 dissociation *per se* was still within the stability margin of the CICR system. However, when both factors concur, the additive sensitization of RyRs causes chaotic  $\text{Ca}^{2+}$  waves in most cells, indicating that the sensitization of RyRs have stepped beyond the stability margin of the CICR system. Once inter-CRU CICR is enabled due to over-sensitization of RyRs, the intracellular  $\text{Ca}^{2+}$  release runs out-of-control, and  $\text{Ca}^{2+}$  waves occur in a

regenerative manner. The chaotic  $\text{Ca}^{2+}$  waves not only prevent cardiomyocytes from rhythmic contraction and relaxation but also activate  $\text{Na}^+/\text{Ca}^{2+}$  exchange and lead to arrhythmogenic excitation.<sup>59</sup> Therefore, preventing RyRs from the wave generation is a prerequisite for the healthy operation of heart cells. The FKBP12.6-mediated suppression of RyR sensitivity is a key mechanism to keep the CICR system from wave generation and cardiac arrhythmia, allowing an indispensable stability margin for dynamic regulation of blood pumping power.

## 5. Limitations

The constitutive FKBP12.6 knockout mouse model has limitations for this study, since the chronic knockout might bring adaptive or compensatory effect. Recently, it has been reported that aged FKBP12.6 knockout mice (1-year old) develop cardiac dysfunction due to the activation of the AKT/mTOR pathway.<sup>35</sup> Although the above activation has not been detected at the age of 3-month-old mice as the same age we used in the present study, we should be cautious that other adaptation might occur. Although we used FK506/rapamycin to acutely dissociate FKBP12.6 from RyRs in order to exclude any adaptive effect that might be brought about by the constitutive knockout of FKBP12.6, there was still limitation, because FK506/rapamycin also dissociates FKBP12. The perfect model for this study is cardiac-specific conditional FKBP12.6 knockout animal. Unfortunately, this model has not been available yet.

## Supplementary material

Supplementary material is available at *Cardiovascular Research* online.

## Acknowledgements

We thank Dr. Xue-Mei Hao for professional technical support and Dr. Iain C. Bruce for editing.

## Funding

This study was supported by the State Major Research and Development Program (2016YFA0500401), National Natural Science Foundation of China (31271228, 31630035, 81370203, 81461148026, and 31327901), the Project of Beijing Municipal Science and Technology Commission (Z14110000214006) and the National Institutes of Health, USA (NIH R01 TW007269).

**Conflict of interest:** None declared.

## References

- Berridge MJ, Dupont G. Spatial and temporal signalling by calcium. *Curr Opin Cell Biol* 1994;**6**:267–274.
- Bers DM. Cardiac excitation-contraction coupling. *Nature* 2002;**415**:198–205.
- Fabiato A, Fabiato F. Contractions induced by a calcium-triggered release of calcium from the sarcoplasmic reticulum of single skinned cardiac cells. *J Physiol* 1975;**249**:469–495.
- Lopez-Lopez JR, Shacklock PS, Balke CW, Wier WG. Local calcium transients triggered by single L-type calcium channel currents in cardiac cells. *Science* 1995;**268**:1042–1045.
- Cheng H, Lederer WJ, Cannell MB. Calcium sparks: elementary events underlying excitation-contraction coupling in heart muscle. *Science* 1993;**262**:740–744.
- Cheng H, Lederer WJ. Calcium sparks. *Physiol Rev* 2008;**88**:1491–1545.
- Guo T, Gillespie D, Fill M. Ryanodine receptor current amplitude controls  $\text{Ca}^{2+}$  sparks in cardiac muscle. *Circ Res* 2012;**111**:28–36.
- Zhao YT, Valdivia HH.  $\text{Ca}^{2+}$  nanosparks: shining light on the dyadic cleft but missing the intensity of its signal. *Circ Res* 2014;**114**:396–398.
- Stern MD. Theory of excitation-contraction coupling in cardiac muscle. *Biophys J* 1992;**63**:497–517.
- Wier WG, Egan TM, Lopez-Lopez JR, Balke CW. Local control of excitation-contraction coupling in rat heart cells. *J Physiol* 1994;**474**:463–471.
- Santana LF, Cheng H, Gomez AM, Cannell MB, Lederer WJ. Relation between the sarcoplasmic  $\text{Ca}^{2+}$  current and  $\text{Ca}^{2+}$  sparks and local control theories for cardiac excitation-contraction coupling. *Circ Res* 1996;**78**:166–171.
- Franzini-Armstrong C, Protasi F, Ramesh V. Shape, size, and distribution of  $\text{Ca}^{2+}$  release units and couplons in skeletal and cardiac muscles. *Biophys J* 1999;**77**:1528–1539.
- Timerman AP, Onoue H, Xin HB, Barg S, Copello J, Wiederrecht G, Fleischer S. Selective binding of FKBP12.6 by the cardiac ryanodine receptor. *J Biol Chem* 1996;**271**:20385–20391.
- Lam E, Martin MM, Timerman AP, Sabers C, Fleischer S, Lukas T, Abraham RT, O'Keefe SJ, O'Neill EA, Wiederrecht GJ. A novel FK506 binding protein can mediate the immunosuppressive effects of FK506 and is associated with the cardiac ryanodine receptor. *J Biol Chem* 1995;**270**:26511–26522.
- Marx SO, Reiken S, Hisamatsu Y, Jayaraman T, Burkhoff D, Roseblit N, Marks AR. PKA phosphorylation dissociates FKBP12.6 from the calcium release channel (ryanodine receptor): defective regulation in failing hearts. *Cell* 2000;**101**:365–376.
- Prestle J, Janssen PM, Janssen AP, Zeitz O, Lehnart SE, Bruce L, Smith GL, Hasenfuss G. Overexpression of FK506-binding protein FKBP12.6 in cardiomyocytes reduces ryanodine receptor-mediated  $\text{Ca}^{2+}$  leak from the sarcoplasmic reticulum and increases contractility. *Circ Res* 2001;**88**:188–194.
- Houser SR. Role of RyR2 phosphorylation in heart failure and arrhythmias: protein kinase A-mediated hyperphosphorylation of the ryanodine receptor at serine 2808 does not alter cardiac contractility or cause heart failure and arrhythmias. *Circ Res* 2014;**114**:1320–1327.
- Kaftan E, Marks AR, Ehrlich BE. Effects of rapamycin on ryanodine receptor/ $\text{Ca}^{2+}$ -release channels from cardiac muscle. *Circ Res* 1996;**78**:990–997.
- Xiao RP, Valdivia HH, Bogdanov K, Valdivia C, Lakatta EG, Cheng H. The immunophilin FK506-binding protein modulates  $\text{Ca}^{2+}$  release channel closure in rat heart. *J Physiol* 1997;**500**(Pt 2):343–354.
- Xin HB, Senbonmatsu T, Cheng DS, Wang YX, Copello JA, Ji GJ, Collier ML, Deng KY, Jeyakumar LH, Magnuson MA, Inagami T, Kotlikoff MJ, Fleischer S. Oestrogen protects FKBP12.6 null mice from cardiac hypertrophy. *Nature* 2002;**416**:334–338.
- Barg S, Copello JA, Fleischer S. Different interactions of cardiac and skeletal muscle ryanodine receptors with FK-506 binding protein isoforms. *Am J Physiol* 1997;**272**:C1726–C1733.
- Xiao J, Tian X, Jones PP, Bolstad J, Kong H, Wang R, Zhang L, Duff HJ, Gillis AM, Fleischer S, Kotlikoff M, Copello JA, Chen SR. Removal of FKBP12.6 does not alter the conductance and activation of the cardiac ryanodine receptor or the susceptibility to stress-induced ventricular arrhythmias. *J Biol Chem* 2007;**282**:34828–34838.
- Doi M, Yano M, Kobayashi S, Kohno M, Tokuhisa T, Okuda S, Suetsugu M, Hisamatsu Y, Ohkusa T, Matsuzaki M. Propranolol prevents the development of heart failure by restoring FKBP12.6-mediated stabilization of ryanodine receptor. *Circulation* 2002;**105**:1374–1379.
- Wehrens XH, Lehnart SE, Huang F, Vest JA, Reiken SR, Mohler PJ, Sun J, Guatimosim S, Song LS, Roseblit N, D'Armiento JM, Napolitano C, Memmi M, Priori SG, Lederer WJ, Marks AR. FKBP12.6 deficiency and defective calcium release channel (ryanodine receptor) function linked to exercise-induced sudden cardiac death. *Cell* 2003;**113**:829–840.
- Zhao YT, Valdivia CR, Gurrola GB, Hernández JJ, Valdivia HH. Arrhythmogenic mechanisms in ryanodine receptor channelopathies. *Sci China Life Sci* 2015;**58**:54–58.
- Stange M, Xu L, Balshaw D, Yamaguchi N, Meissner G. Characterization of recombinant skeletal muscle (Ser-2843) and cardiac muscle (Ser-2809) ryanodine receptor phosphorylation mutants. *J Biol Chem* 2003;**278**:51693–51702.
- Xiao B, Sutherland C, Walsh MP, Chen SR. Protein kinase A phosphorylation at serine-2808 of the cardiac  $\text{Ca}^{2+}$ -release channel (ryanodine receptor) does not dissociate 12.6-kDa FK506-binding protein (FKBP12.6). *Circ Res* 2004;**94**:487–495.
- McCall E, Li L, Satoh H, Shannon TR, Blatter LA, Bers DM. Effects of FK-506 on contraction and  $\text{Ca}^{2+}$  transients in rat cardiac myocytes. *Circ Res* 1996;**79**:1110–1121.
- Zhang X, Tallini YN, Chen Z, Gan L, Wei B, Doran R, Miao L, Xin HB, Kotlikoff MJ, Ji G. Dissociation of FKBP12.6 from ryanodine receptor type 2 is regulated by cyclic ADP-ribose but not beta-adrenergic stimulation in mouse cardiomyocytes. *Cardiovasc Res* 2009;**84**:253–262.
- Wang LG. Near-atomic resolution structure of the largest known  $\text{Ca}^{2+}$  channel: ryanodine receptor. *Sci China Life Sci* 2015;**58**:221–222.
- Efremov RG, Leitner A, Aebersold R, Rausner S. Architecture and conformational switch mechanism of the ryanodine receptor. *Nature* 2015;**517**:39–43.
- Zalk R, Clarke OB, des Georges A, Grassucci RA, Reiken S, Mancia F, Hendrickson WA, Frank J, Marks AR. Structure of a mammalian ryanodine receptor. *Nature* 2015;**517**:44–49.
- Yan Z, Bai XC, Yan C, Wu J, Li Z, Xie T, Peng W, Yin CC, Li X, Scheres SH, Shi Y, Yan N. Structure of the rabbit ryanodine receptor RyR1 at near-atomic resolution. *Nature* 2015;**517**:50–55.
- Peng W, Shen H, Wu J, Guo W, Pan X, Wang R, Chen SR, Yan N. Structural basis for the gating mechanism of the type 2 ryanodine receptor RyR2. *Science* 2016;**354**:aah5324-1-10.

35. Yuan Q, Chen Z, Santulli G, Gu L, Yang ZG, Yuan ZQ, Zhao YT, Xin HB, Deng KY, Wang SQ, Ji G. Functional role of Calstabin2 in age-related cardiac alterations. *Sci Rep* 2014;**4**:7425.
36. Xu M, Zhou P, Xu SM, Liu Y, Feng X, Bai SH, Bai Y, Hao XM, Han Q, Zhang Y, Wang SQ. Intermolecular failure of L-type Ca<sup>2+</sup> channel and ryanodine receptor signaling in hypertrophy. *PLoS Biol* 2007;**5**:e21.
37. Zhou P, Zhao YT, Guo YB, Xu SM, Bai SH, Lakatta EG, Cheng H, Hao XM, Wang SQ. Beta-adrenergic signaling accelerates and synchronizes cardiac ryanodine receptor response to a single L-type Ca<sup>2+</sup> channel. *Proc Natl Acad Sci U S A* 2009;**106**:18028–18033.
38. Wang SQ, Song LS, Lakatta EG, Cheng H. Ca<sup>2+</sup> signalling between single L-type Ca<sup>2+</sup> channels and ryanodine receptors in heart cells. *Nature* 2001;**410**:592–596.
39. Torres NS, Larbig R, Rock A, Goldhaber JL, Bridge JH. Na<sup>+</sup> currents are required for efficient excitation-contraction coupling in rabbit ventricular myocytes: a possible contribution of neuronal Na<sup>+</sup> channels. *J Physiol* 2010;**588**:4249–4260.
40. Xin HB, Rogers K, Qi Y, Kanematsu T, Fleischer S. Three amino acid residues determine selective binding of FK506-binding protein 12.6 to the cardiac ryanodine receptor. *J Biol Chem* 1999;**274**:15315–15319.
41. Guo T, Cornea RL, Huke S, Camors E, Yang Y, Picht E, Fruen BR, Bers DM. Kinetics of FKBP12.6 binding to ryanodine receptors in permeabilized cardiac myocytes and effects on Ca sparks. *Circ Res* 2010;**106**:1743–1752.
42. Su Z, Sugishita K, Li F, Ritter M, Barry WH. Effects of FK506 on [Ca<sup>2+</sup>]<sub>i</sub> differ in mouse and rabbit ventricular myocytes. *J Pharmacol Exp Ther* 2003;**304**:334–341.
43. Liu J, Farmer JD Jr, Lane WS, Friedman J, Weissman I, Schreiber SL. Calcineurin is a common target of cyclophilin-cyclosporin A and FKBP-FK506 complexes. *Cell* 1991;**66**:807–815.
44. Samso M, Shen X, Allen PD. Structural characterization of the RyR1-FKBP12 interaction. *J Mol Biol* 2006;**356**:917–927.
45. Oda T, Yang Y, Uchinoumi H, Thomas DD, Chen-Izu Y, Kato T, Yamamoto T, Yano M, Cornea RL, Bers DM. Oxidation of ryanodine receptor (RyR) and calmodulin enhance Ca release and pathologically alter, RyR structure and calmodulin affinity. *J Mol Cell Cardiol* 2015;**85**:240–248.
46. Seidler T, Loughrey CM, Zibrova D, Kettlewell S, Teucher N, Kogler H, Hasenfuss G, Smith GL. Overexpression of FK-506 binding protein 12.0 modulates excitation contraction coupling in adult rabbit ventricular cardiomyocytes. *Circ Res* 2007;**101**:1020–1029.
47. Galfre E, Pitt SJ, Venturi E, Sitsapesan M, Zaccai NR, Tsaneva-Atanasova K, O'Neill S, Sitsapesan R. FKBP12 activates the cardiac ryanodine receptor Ca<sup>2+</sup>-release channel and is antagonised by FKBP12.6. *PLoS One* 2012;**7**:e31956.
48. Loughrey CM, Seidler T, Miller SL, Prestle J, MacEachern KE, Reynolds DF, Hasenfuss G, Smith GL. Over-expression of FK506-binding protein FKBP12.6 alters excitation-contraction coupling in adult rabbit cardiomyocytes. *J Physiol* 2004;**556**:919–934.
49. Gomez AM, Schuster I, Fauconnier J, Prestle J, Hasenfuss G, Richard S. FKBP12.6 overexpression decreases Ca<sup>2+</sup> spark amplitude but enhances [Ca<sup>2+</sup>]<sub>i</sub> transient in rat cardiac myocytes. *Am J Physiol Heart Circ Physiol* 2004;**287**:H1987–H1993.
50. Huang F, Shan J, Reiken S, Wehrens XH, Marks AR. Analysis of calstabin2 (FKBP12.6)-ryanodine receptor interactions: rescue of heart failure by calstabin2 in mice. *Proc Natl Acad Sci U S A* 2006;**103**:3456–3461.
51. Gellen B, Fernandez-Velasco M, Briec F, Vinet L, LeQuang K, Rouet-Benzineb P, Benitah JP, Pezet M, Palais G, Pellegrin N, Zhang A, Perrier R, Escoubet B, Marniquet X, Richard S, Jaisser F, Gomez AM, Charpentier F, Mercadier JJ. Conditional FKBP12.6 overexpression in mouse cardiac myocytes prevents triggered ventricular tachycardia through specific alterations in excitation-contraction coupling. *Circulation* 2008;**117**:1778–1786.
52. Previlon M, Pezet M, Semprez F, Mercadier JJ, Rouet-Benzineb P. FKBP12.6 mice display temporal gender differences in cardiac Ca(2+)-signalling phenotype upon chronic pressure overload. *Can J Physiol Pharmacol* 2011;**89**:769–782.
53. Vinet L, Pezet M, Bito V, Briec F, Biesmans L, Rouet-Benzineb P, Gellen B, Previlon M, Chimenti S, Vilaine JP, Charpentier F, Sipido KR, Mercadier JJ. Cardiac FKBP12.6 overexpression protects against triggered ventricular tachycardia in pressure overloaded mouse hearts. *Basic Res Cardiol* 2012;**107**:246.
54. Bito V, Biesmans L, Gellen B, Antoons G, Macquade N, Rouet-Benzineb P, Pezet M, Mercadier JJ, Sipido KR. FKBP12.6 overexpression does not protect against remodeling after myocardial infarction. *Exp Physiol* 2013;**98**:134–148.
55. Rios E, Stern MD. Calcium in close quarters: microdomain feedback in excitation-contraction coupling and other cell biological phenomena. *Annu Rev Biophys Biomol Struct* 1997;**26**:47–82.
56. Soeller C, Crossman D, Gilbert R, Cannell MB. Analysis of ryanodine receptor clusters in rat and human cardiac myocytes. *Proc Natl Acad Sci U S A* 2007;**104**:14958–14963.
57. Baddeley D, Jayasinghe ID, Lam L, Rossberger S, Cannell MB, Soeller C. Optical single-channel resolution imaging of the ryanodine receptor distribution in rat cardiac myocytes. *Proc Natl Acad Sci U S A* 2009;**106**:22275–22280.
58. Inoue M, Bridge JH. Ca<sup>2+</sup> sparks in rabbit ventricular myocytes evoked by action potentials: involvement of clusters of L-type Ca<sup>2+</sup> channels. *Circ Res* 2003;**92**:532–538.
59. Boyden PA, Barbaiya C, Lee T, ter Keurs HE. Nonuniform Ca<sup>2+</sup> transients in arrhythmogenic Purkinje cells that survive in the infarcted canine heart. *Cardiovasc Res* 2003;**57**:681–693.